University of Baghdad
College of Engineering
JOURNAL OF ENGINEERING

Journal of Engineering

journal homepage: www.jcoeng.edu.iq
Number 3 Volume 24 March 2018

Mechanical and Energy Engineering

Numerical Simulation of Thermal-Hydrodynamic Behavior within Solar Air Collector

Mustafa T. Mustafa
Assistant Professor
Technical Engineering College, Middle Technical University
drmustafa6087@yahoo.com

Ayad T. Mustafa
Lecturer
College of Engineering, Al-Nahrain University
ayad_altai@yahoo.com

ABSTRACT

Solar collectors, in general, are utilized to convert the solar energy into heat energy, where it is employed to generate electricity. The non-concentrating solar collector with a circular shape was adopted in the present study. Ambient air is heated under a translucent roof where buoyant air is drawn from outside periphery towards the collector center (tower base). The present study is aimed to predict and visualize the thermal-hydrodynamic behavior for airflow under inclined roof of the solar air collector, SAC. Three-dimensional of the SAC model using the re-normalization group, RNG, $k-\varepsilon$ turbulence viscus model is simulated. The simulation was carried out by using ANSYS-FLUENT 14.5. The simulation results demonstrated that at same insolation; airflow, ground and air temperatures increase when the collector radius decreases towards the collector center. The ground temperature and air velocity increase, while airflow temperature decreases when the inclination angle increases from 0° to 20° due to changing in airflow movement. More decreasing in airflow temperature has been occurred when the inlet height increases from 0.1m to 0.25m. The simulation results were validated by comparing with the experimental data. In conclusions, the obtained results showed the capability of producing warm airflow to generate electricity in Baghdad city.

Key words: numerical simulation; thermal-hydrodynamic analysis; solar collector; solar load model; energy conversion.

المحاكاة العددية للسلوك الحراري الهيدروديناميكي داخل مجمع الهواء الشمسي

أ.م.د. مصطفى طارق مصطفى
الكلية التقنية الهندسية/الجامعة التقنية الوسطى

م.د. اياد طارق مصطفى
كلية الهندسة/جامعة النهرين

الخلاصة

تستخدم المجمعات الشمسية, بشكل عام, لتحويل الطاقة الشمسية إلى طاقة حرارية, حيث ينتفع بها لتوليد الكهرباء. المجمع الشمسي الغير التركيزي ذو الشكل الدائري هو الذي اعتمد في الدراسة الحالية. يتم تسخين الهواء المحيط تحت مظلة شفافة حيث يسحب الهواء الطافي من المحيط الخارجي نحو مركز المجمع (قاعدة البرج). تهدف الدراسة الحالية إلى تنبؤ واظهار السلوك الحراري-الهيدروديناميكي لتدفق الهواء تحت سقف مائل لمجمع هواء شمسي. نموذج مجمع الهواء الشمسي باستخدام نموذج اللزوجة المضطرب RNG $k-\varepsilon$ تم محاكاته. تم تنفيذ المحاكاة باستخدام ANSYS FLUENT 14.5. أظهرت نتائج المحاكاة أنه لنفس الاشعاع الشمسي: تدفق الهواء, درجة حرارة الهواء والارض تزداد عندما يتناقص نصف قطر المجمع تجاه مركزه. درجات

حرارة الارض وسرعة الهواء تزداد, بينما درجات حرارة الهواء تنخفض عندما تزداد زاوية الميل من °0 الى °20 نتيجة لتغير حركة تدفق الهواء. انخفاض اكثر في درجات حرارة الهواء حدث عندما ازداد ارتفاع مدخل المجمع من 0.1 م الى 0.25 م. تم التحقق من صحة نتائج المحاكاة بالمقارنة مع البيانات التجريبية. كشفت الاستنتاجات من النتائج المستخلصة على مقدرة الهواء الساخن المنتج من المجمع الشمسي على توليد الكهرباء في مدينة بغداد.

الكلمات الرئيسية: المحاكاة العددية, التحليل الحراري الهيدروديناميكي, المجمع الشمسي, نموذج الحمل الشمسي, تحويل الطاقة.

1. INTRODUCTION

The solar radiation can be utilized to heating natural airflow within a transparent system. The solar air heating system has advantages of simple construction and maintenance, moreover less corrosion compared with solar water heating system. The solar air heating system is called solar air collector, SAC. Solar air collectors are receivers of solar radiation that is used to convert it to heat energy. Generally speaking, solar collectors are either non-concentrating or concentrating solar radiation. SAC, of non-concentrating type, has a transparent area equivalent to the absorber area. An application for the SAC, a solar updraft tower plant that uses hot air extracted from the SAC to generate electricity by a wind turbine. The SAC utilizes heating technique based on the solar absorbing at the base then airflow heating through heat picks up from the absorber, **Mustafa, et al., 2015**.

Heat transfer and flow field in the solar collector were studied numerically by means of computational fluid dynamics, CFD, and investigated experimentally through a solar collector panel of 12.5 m^2 in area and 16 parallel horizontal fins. The solar collector panel was investigated in two methods; 1st with an absorber consisting of horizontally inclined strips by **Jianhua, et al., 2007**, and 2nd with an absorber consisting of horizontal fins by **Jianhua, et al., 2005**. Temperature measurements were utilized to validate the flow distribution through the absorber pipes. When high glycol flow rate is used, distribution flow via the fins absorber is uniform. Worst result of the flow distribution in the upper part of the collector panel was obtained when the collector tilt and inlet temperature increased, and the glycol flow rate decreased.

The performance of the unglazed transpired solar collector, UTC, was simulated numerically with computational fluid dynamics CFD tools. **Wang, et al., 2006**, compared numerically UTC with several kinds of traditional solar air collectors. Whilst **Li, et al., 2013**, simulated the convective heat transfer process for both flat and corrugated UTC. The results showed that the UTC have advantages in the ventilation and heating fields, a significant method in corrugated UTC was used by combination the effects of corrugation geometry and incident turbulence intensity. **Fasel**, **et al**., **2012,** and **Hermann**, **et al**., **2013**, employed computational fluid dynamics CFD for investigating the solar chimney power plant, SCPP. The geometric dimensions effect on thermo-fluid dynamics and the power output were investigated. As result to increasing the heat transfer coefficient, the collector efficiency was revealed to improve with increasing SCPP scale, i.e. the solar collector dimensions.

The airflow nature through the duct of a solar air heater with Reynolds number effects ranging from 3000 to 18000 on Nusselt number was investigated. CFD simulation was carried out for the investigation with absorber plate having; triangular rib roughness by **Yadav** and **Bhagoria 2013**, and for rectangular rib roughness by **Rajpoot**, **2013** and **Chaudhari, et al**., **2014** with double glass sheets. Simulation results revealed that the Nusselt number increases with the increase in Reynolds number, and the temperature increases at the duct outlet due to the rectangular shape of the duct. Numerical simulation for drying foods in the solar collector was carried out. **Ingle**, **et al**., **2013,**

developed a collector for grape drying. The collector model involving air inlet, wavy structured absorber plate, glass cover plate, and pebble block. **Manilal**, **2016** utilized the solar collector for drying food and increment the efficiency. CFD tool has been used to simulate different types of collector plate having different configurations. The results showed that the temperature of collector outlet depends on the solar radiation, where it's directly proportional with irradiance.

An improvement of the solar collector efficiency was carried out by enhancement techniques. **Islamuddin**, **et al**., **2013**, improved the solar chimney power plants by numerical modeling using ANSYS-FLUENT. The collector enhancement uses thermal hybrid technique of hot exhaust gases combined with the solar radiation. The hybrid technique becomes active all the day, and enhances the power output by 38.8 % at 1000 W/m^2 solar irradiation. Another enhancement to the solar collector was carried out by longitudinal baffles above the absorber to extend the flow and reduce the dead zones to a minimum. **Amraoui**, and **Aliane 2014,** simulated the solar collector and study the heat transfer capability, which leads to increasing the efficiency with baffles technique. These baffles act as fins and improve the heat transfer within the solar collector.

Khilkhal, **et al**., **2014**, simulated the solar collector as a part of solar chimney power plant using finite volume technique by ANSYS-FLUENT. The results show that the velocity increases when the collector diameter increases and when the solar radiation is 300, 450, 600, 750 and 900 W/m^2. **Guo, et al**., **2014** predicted numerically that increasing the ambient temperature has evident effect on air velocity. **Mustafa**, **et al**., **2015,** presented mathematical and experimental study for the SAC. Modeling with conservation equations were carried out and model solution is obtained by utilizing a developed code in MATLAB. Experimental concentric circles was designed and fabricated to perform measurements for thermo-fluid process in the system. The canopy inclination of 8.5^o was performed in modeling. The results showed that at same solar irradiation, the temperatures of airflow are increasing by decreasing the radius toward the center, and airflow temperature decreases when the canopy slope increases. When the solar radiation increases, airflow temperature increases for the same collector radius. The model results agree with the experimental results. **Gholamalizadeh** and **Man-Hoe**, **2016** utilized CFD tools for the solar chimney power plant with an inclined collector roof. The effect of the collector configuration on the plant performance was performed. The results showed that when the collector inclination increases, the mass flow rate increases too.

In summary, the previous studies demonstrated numerical simulation by means of computational fluid dynamics CFD were carried out for the SAC. Moreover, mathematical and experimental modeling was employed. Some studies aim to predict the performance of the solar air duct and unglazed transpired solar collector UTC, or to improve the efficiency by enhancement techniques. Other studies analyzed thermo-fluid properties within the solar chimney power plants SCPP, and the configuration of SCPP with an inclined collector roof effects on the plant performance. The main validation to CFD simulations were made by comparing the obtained results with Manzanares prototype data. It is realized that there are gaps in the methods of investigation for thermo-fluid dynamics processes within 3D inclined collector roof of SCPP.

In this paper, numerical simulation has been utilized to investigate thermal-hydrodynamic behavior within the SAC in Baghdad. The simulation of the SAC was carried out for 3D construction with $k-\varepsilon$ viscous model and solar load model by using ANSYS-FLUENT 14.5. The purpose of this study is to predict and visualize heat transfer and flow field within an inclined SAC. The collector roof inclination is modified by increasing the outlet height. A significance of the

present study could show through visualization the flow behavior within the SAC under the effect of changing angles of the collector inclination and the collector height. **Fig. 1** shows a sectional view in the SAC. The analysis of the solar chimney is not in the scope of this paper. Simulation model is validated by comparison with previous experimental data.

2. NUMERICAL SIMULATION

Numerical procedures solve the interacting governing equations in a coupled method by finite volume framework. The modeling is carried out in GAMBIT and subsequently the mesh is imported to ANSYS-FLUENT 14.5 for solving and post processing.

2.1 Modeling in GAMBIT

The modeling is carried out in GAMBIT; a quarter circular configuration of the SAC was built, as shown in **Fig. 2**. The SAC model has the collector ground and inclined roof (glass), which produced an outer peripheral collector inlet and a central collector outlet. Ambient air enters at outer peripheral and heated under a transparent roof by the solar radiation where warm air is drawn towards the collector center. The adopted dimensions of the SAC model are; the radius, *r*, of the collector ground is 5 m, and the radius of the collector outlet is 0.5 m where the rest radius for the roof is 4.5 m. The height, *z*, of collector roof at inlet, at point 1 shown in **Fig. 1**, is varied via 0.1 m and 0.25 m, as the cases described in **Table 1**.

The simulation cases studied in the present research are shown in **Table 1**. The cases can be described by the angle, φ, of the collector roof inclination for two inlet height, 0.1 m and 0.25 m. Angle inclination of the collector roof are 0°, 8.5°, and 20°. Further investigation for the simulation cases were done through different implementation of the solar radiation incident for the same roof inclination, 8.5°, and inlet height, 0.1 m. For this case, the solar radiation, *I*, utilized is: 500, 750, and 1000 W/m^2, as described in **Table 1**.

The geometry of SAC is meshed using tetrahedral/hybrid elements with T-Grid scheme type, as shown in **Fig. 3**, **Jianhua, et al., 2007**. The geometry meshed by spacing interval size of 0.0275, **Khilkhal, et al., 2014**, and number of generated elements for each case is shown in **Table 1**. Then, the mesh was written out in the format used by FLUENT for solving process. For a successful computational work, the boundary types of the SAC geometry were specified. The boundary types utilize for the SAC model are shown in **Table 2**. The solution is considered convergent if the scaled residual for the continuity and the momentum equations are less than 1.0×10^{-3}, k-epsilon and do-intensity equations are less than1.0×10^{-4}, and the energy equation is less than 1.0×10^{-6}. The iterations of convergent solutions for implemented cases are ranged between 1060 and 2900 during period extended to three hours.

2.2 Simulation with FLUENT

Numerical method employed for the SAC model consist of pressure – velocity coupling scheme used in solving the flow problem in a segregated manner, and advanced viscous RNG $k-\varepsilon$ model is considered with standard wall treatment of near wall functions. The RNG based $k-\varepsilon$ turbulence model is derived from the instantaneous Navier-Stokes equations, using a mathematical technique called “Re-Normalization Group” (RNG) methods. The RNG $k-\varepsilon$ model has a similar form to the standard $k-\varepsilon$ model shown in Eqs. (1) and (2) with features. These features make the RNG $k-\varepsilon$

model more accurate and reliable for a wider class of flows than the standard $k-\varepsilon$ model, **ANSYS-FLUENT, 2013**.

$$\frac{\partial}{\partial t}(\rho k)+\frac{\partial}{\partial x_i}(\rho k u_i)=\frac{\partial}{\partial x_j}\left(\zeta_k \mu_{eff}\frac{\partial k}{\partial x_j}\right)+G_k+G_b-\rho\varepsilon-Y_M+S_k \quad (1)$$

$$\frac{\partial}{\partial t}(\rho \varepsilon)+\frac{\partial}{\partial x_i}(\rho \varepsilon u_i)=\frac{\partial}{\partial x_j}\left(\zeta_\varepsilon \mu_{eff}\frac{\partial \varepsilon}{\partial x_j}\right)+C_{1\varepsilon}\frac{\varepsilon}{k}(G_k+C_{3\varepsilon}G_b)-C_{2\varepsilon}\rho\frac{\varepsilon^2}{k}-R_\varepsilon+S_\varepsilon \quad (2)$$

where u_i represents velocity component, G_k is the generation of turbulence kinetic energy due to the mean velocity gradients, G_b is the generation of turbulence kinetic energy due to buoyancy, and Y_M represents the contribution of the fluctuating dilatation in compressible turbulence to the overall dissipation rate.

The radiation model was selected with discrete ordinates, DO, for the position of 44.4 in longitude and 33.3 in latitude, which represent Baghdad city. Then the solar load was activated with DO Irradiation for the solar radiation calculations. The collector roof material for transmitted insolation is the glass, which its properties adapted from **Manilal, 2016**. The current study used different direct solar radiation (500, 750, and 1000 W/m^2). Therefore, the numerical simulation under transient state conditions was studied for one geometry volume. The input parameters used in the simulation cases are airflow temperature and velocity, the solar irradiance, inclination angle of the collector roof, and inlet collector height. Meanwhile, numerical simulation of the SAC was carried out successfully by comparing its results with experimental data that obtained by **Mustafa, et al., 2015,** at the same inlet collector height, inclination angle, and collector radius.

3. RESULTS AND DISCUSSIONS

Results of numerical simulation for the SAC were obtained, different simulation cases in Baghdad location were carried out. Thermal and flow field distribution within the SAC model will be presented in contours shape, and then discussed. Numerical results have been compared with previous experimental data.

3.1 Thermal Analysis

Thermal phenomenon occurs in the SAC based on irradiance absorbability of the collector ground, and then emitted to the fluid flow. Therefore, temperature of airflow increases with collector radius decreasing from the collector inlet towards the center. For simulation model with collector radius of 5 m, temperature distribution results of the ground are shown in **Fig. 4** for an inlet height of 0.1 m with different inclination angle. The simulation results show the ground temperature distribution increase with collector radius decreasing towards the center. Furthermore, the ground temperature distribution increases with inclination angle increase from 0° to 20° for the same solar radiation of 1000 W/m^2. Whilst, airflow temperature distribution decreases when inclination angle increases from 0° to 20° for the same solar radiation, as shown in **Fig. 5**. These results dates back to still air under the collector roof when inclination angle is 0°, then when inclination angle increases airflow movement also increases due to free convection. Results of **Fig. 5** are in agreement with obtained results by **Mustafa, et al., 2015**. Further detraction in airflow temperature is shown in **Fig. 6**. The figure shows distribution of airflow temperature decreases

when inlet height increases from 0.1 m to 0.25 m with different inclination angle and same solar radiation.

3.2 Flow Analysis

The solar energy is converted to heat energy under a transparent roof of the SAC, where part of the heat energy converts to kinetic energy. Airflow moves towards the collector outlet due to the kinetic energy. Therefore, velocity of airflow increases with collector radius decreasing from the collector inlet towards the center. **Fig. 7** shows velocity distribution of airflow for the SAC model of 5 m in radius, solar radiation of 1000 W/m^2, inclination angle of 0°, and different inlet heights. The simulation results show the velocity distribution increases with collector radius decreasing towards the center, while slightly increases with clear contours arrangement when inlet height increases to 0.25 m. Other results reveal in **Fig. 8** for inclination angle of 8.5° with the same parameters used in simulation results shown in **Fig. 7**. The figure shows increase in airflow velocity towards the collector outlet in comparison with the results of 0° inclination angle. Airflow increment dates back to changing in the heat energy to the kinetic energy. Airflow increases until maximum radiation absorption at a tilt angle that correspond the collector location latitude. Airflow increases when inclination angle increase is in agreement with obtained results by **Gholamalizadeh** and **Man-Hoe, 2016**. Therefore, the power generation increases due to increasing warm airflow rate, as revealed by **Guo, et al**., **2014**.

The solar irradiance is one of the input parameters to the SAC simulation. Hence, when insolation increases through different simulation cases (500, 750, and 1000 W/m^2), temperature of warm air under transparent roof increase too. The temperature of warm air increases due to increasing of ground temperature. Moreover, flow rate of warm air increase when the solar radiation increases due to, slightly, increasing velocity of warm air.

3.3 Validation of Numerical Simulation

Numerical results have been validated by comparing outcomes with experimental data that obtained by **Mustafa, et al., 2015**. The comparison has been carried out at the experimental measurements conditions. Airflow temperatures of the SAC model have been compared numerically and experimentally, as shown in **Fig. 9**. The comparison included air temperature difference between outlet and inlet. The mean percentage of temperature difference in compared results is 5.7%.

4. CONCLUSIONS

Airflow within the SAC is simulated using ANSYS-FLUENT 14.5 with preprocessing using GAMBIT 2.4.6. The simulation was carried out for 3D, $k-\varepsilon$ viscous, and solar load models. Thermo–fluid dynamic analysis of the SAC was visualized through numerical simulation. Simulation results of case study are validated by comparison with the experimental data. The conclusions drawn from simulation results are:

1. The ground and airflow temperatures increase when collector radius decreasing towards the collector center. When inclination angle increases from 0° to 20° for the same solar radiation incidence, the ground temperatures increase while airflow temperatures decrease. Decreasing airflow temperatures dates back to changing in airflow movement. More

detraction in airflow temperatures has been occurred when inlet height increases from 0.1 m to 0.25 m for the same solar radiation incidence.

2. Air velocity increases with collector radius decreasing towards the collector center. Moreover, air velocity increases when inlet height increase from 0.1 m to 0.25 m and when inclination angle increase from 0° to 8.5° for the same solar radiation incidence. Flow increment dates back to changing the heat energy to kinetic energy.
3. Warm air temperatures and flow rate increase when the solar radiation increases for the same collector radius.
4. Increasing production of warm airflow from the SAC capable of spin the wind turbine and generates electricity.
5. The match between the simulation results is acceptable compared with the previous experimental results. The mean percentage of temperature difference in compered results is 5.7%.

REFERENCES

- Amraoui. M. A., Aliane. K., 2014, *Numerical analysis of a three dimensional fluid flow in a flat plate solar collector*, International Journal of Renewable and Sustainable Energy, 3(3): 68-75.

- ANSYS-FLUENT, 2013, *Theory Guide Release R14.5*, ANSYS, Inc.

- Chaudhari, Sohel, Mukesh Makwana, Rajesh Choksi, and Gaurav Patel, 2014, *CFD Analysis of Solar Air Heater*, International Journal of Engineering Research and Applications 4, no. 6: 47-50p.

- Fasel, Hermann F., Ehsan Shams, and Andreas Gross, 2012, *CFD analysis for solar chimney power plants*, 9th International Conference on Heat Transfer, Fluid Mechanics and Thermodynamics.

- Gholamalizadeh, Ehsan, and Man-Hoe Kim, 2016, *CFD (computational fluid dynamics) analysis of a solar-chimney power plant with inclined collector roof*, Energy 107: 661-667.

- Guo, Peng-hua, Jing-yin Li, and Yuan Wang, 2014, *Numerical simulations of solar chimney power plant with radiation model*, Renewable energy, 62: 24-30.

- Hermann F., Fanlong Meng, Ehsan Shams, and Andreas Gross, 2013, *CFD analysis for solar chimney power plants*, Solar Energy, 98: 12-22.

- Ingle, P. W., A. A. Pawar, B. D. Deshmukh, and K. C. Bhosale, 2013, *CFD analysis of solar flat plate collector*, International Journal of Emerging Technology and Advanced Engineering, 3, no. 4: 337-342.

- Islamuddin, Azeemuddin, Hussain H. Al-Kayiem, and Syed I. Gilani, 2013, *Simulation of solar chimney power plant with an external heat source*, IOP Conference Series: Earth and Environmental Science, Vol. 16. No. 1, IOP Publishing.

- Jianhua Fan, Louise Jivan Shah, and Simon Furbo, 2005, *Flow distribution in a solar collector panel with horizontal fins*, Proceedings of the 2005 Solar World Congress.
- Jianhua Fan, Louise Jivan Shah, and Simon Furbo, 2007, *Flow distribution in a solar collector panel with horizontally inclined absorber strips*, Solar Energy 81.12: 1501-1511.
- Khilkhal A. Husain, Shate W. M., and Jassim A. J., 2014, *Numerical Simulation of The Influence of Geometric Parameter on The Flow Behavior in a Solar Chimney Power Plant system*, Journal of Engineering, No. 8, Vol. 20.
- Li S., Karava P., Savory E. and Lin W. E., 2013, *CFD Simulations for Thermal and Airflow Analysis of Unglazed Transpired Solar Collectors*, 6th European and African Conference on Wind Engineering.
- Manilal, Kumavat Mukesh, 2016, *Design, CFD Analysis and Fabrication of Solar Flat Plate Collector*, International Research Journal of Engineering and Technology.
- Mustafa A. T., Al-Kayiem H. H. and Gilani I. U., 2015, *Investigation and Evaluation of the Solar Air Collector Model to Support the Solar Vortex Engine*, ARPN Journal of Engineering and Applied Sciences, Vol. 10, No. 12.
- Rajpoot, Surjeet Singh, and Dinesh Kumar Koli, 2013, *CFD analysis of solar air heater duct with rectangular rib surface*, International Journal of Engineering Trends and Technology, 1.4: 3006-3011.
- Wang, C., Guan, Z., Zhao, X. and Wang, D., 2006, *Numerical simulation study on transpired solar air collector*, Renewable Energy Resources and a Greener Future Vol.VIII-3-4, ICEBO.

- Yadav, Anil Singh, and J. L. Bhagoria, 2013, *A CFD analysis of a solar air heater having triangular rib roughness on the absorber plate*, International Journal of ChemTech Research, 5.2: 964-971.

NOMENCLATURE AND ABBREVIATIONS

Symbol	Description	Unit
I	solar radiation	W/m^2
r	radial coordinate directed	
u_i	velocity component	m/s
z	axial coordinate direction	
ρ	density	kg/m^3
θ	circumferential coordinate direction	
φ	inclination angle	degree
CFD	computational fluid dynamics	
DO	discrete ordinates	
RNG	renormalization group	
SAC	solar air collector	
SCPP	solar chimney power plant	
UTC	unglazed transpired solar collector	

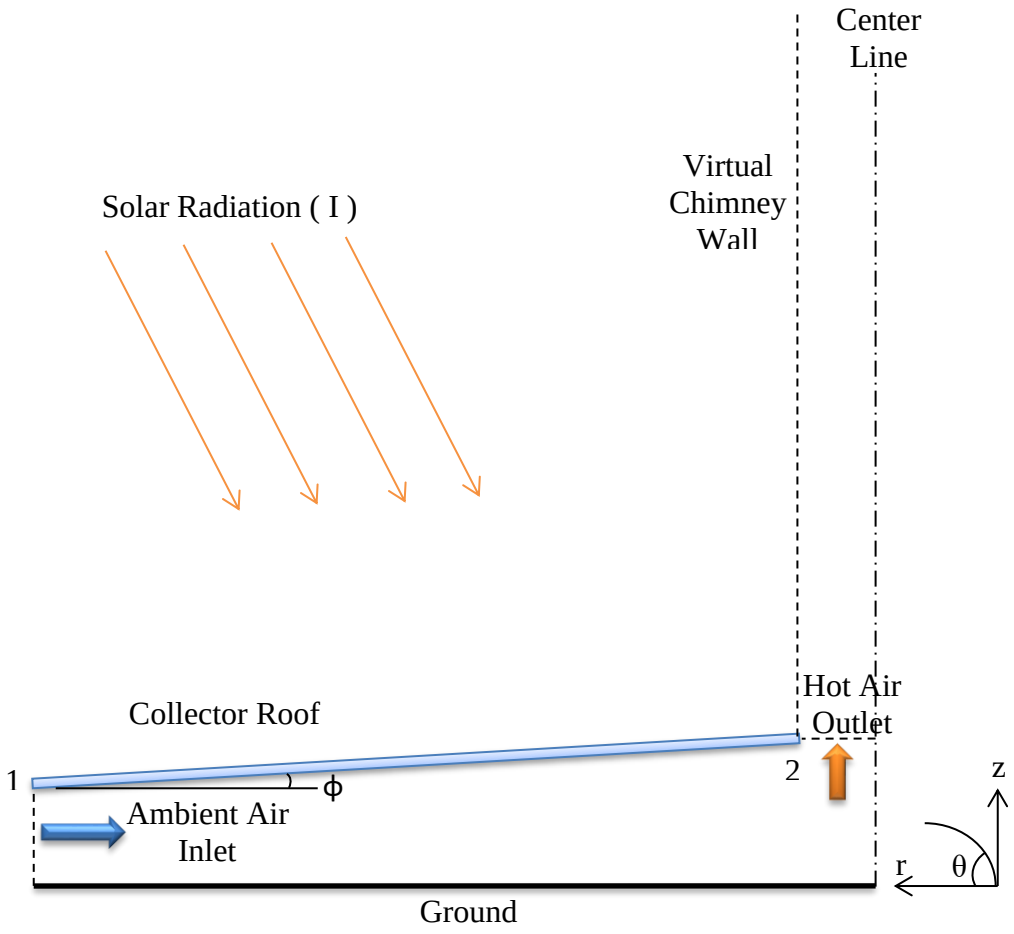

Figure 1. Sectional view in the SAC.

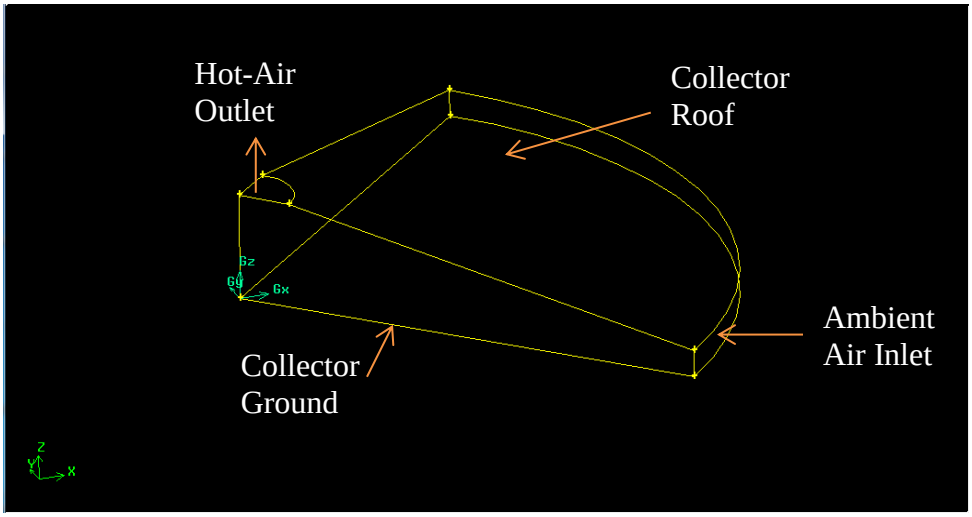

Figure 2. Configuration of the SAC model in GAMBIT.

Table 1. Case-Meshing properties of the SAC model.

Case No.	Collector Roof Angle, ϕ (degree)	No. of Mesh Elements	Solar Radiation Incidence (W/m^2)	Collector Inlet Height, z (m)
1	0°	611564	1000	0.1
2	8.5°	1465661	1000	
			750	
			500	
3	20°	2931385	1000	
1	0°	1528910	1000	0.25
2	8.5°	2383007		

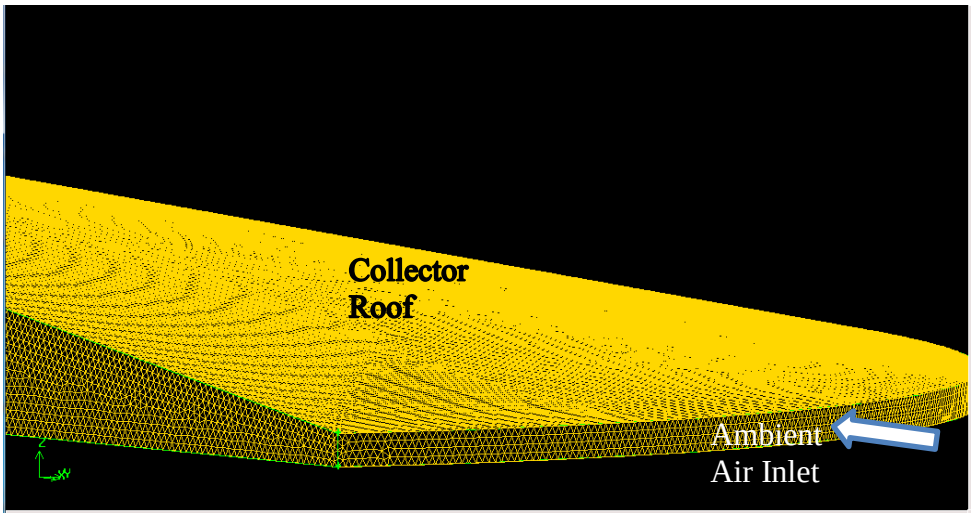

Figure 3. Tetrahedral mesh quality of the SAC model.

Table 2. Boundary types for the SAC model.

Boundary	Type	Boundary Properties
Ground (soil)	Stationary wall	Opaque
Roof (glass)	Stationary wall	Semi-transparent: Radiation-Discrete Ordinates (DO)
Collector inlet	Velocity-inlet	Constant air temperature and velocity
Collector outlet	Outflow	External black body temperature method: Boundary temperature
The collector sides	Stationary wall	Symmetry

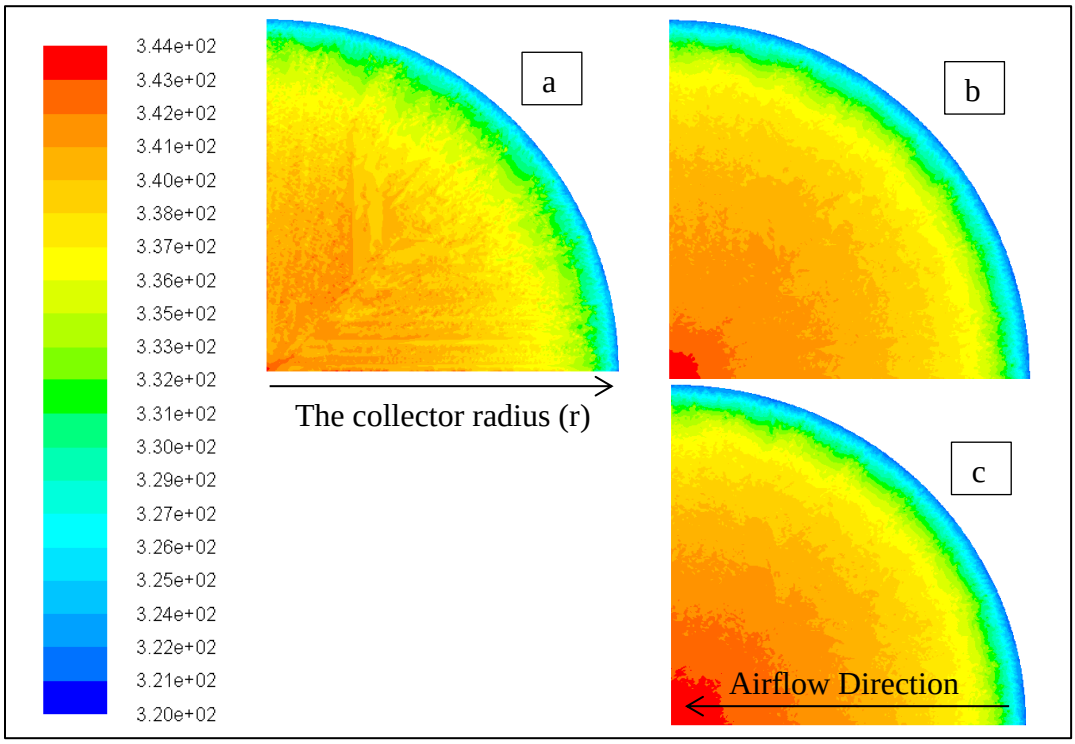

Figure 4. Temperature gradient of the SAC ground in (K) with inlet height of 0.1 m and inclination angle of (a) 0°, (b) 8.5°, and (c) 20°.

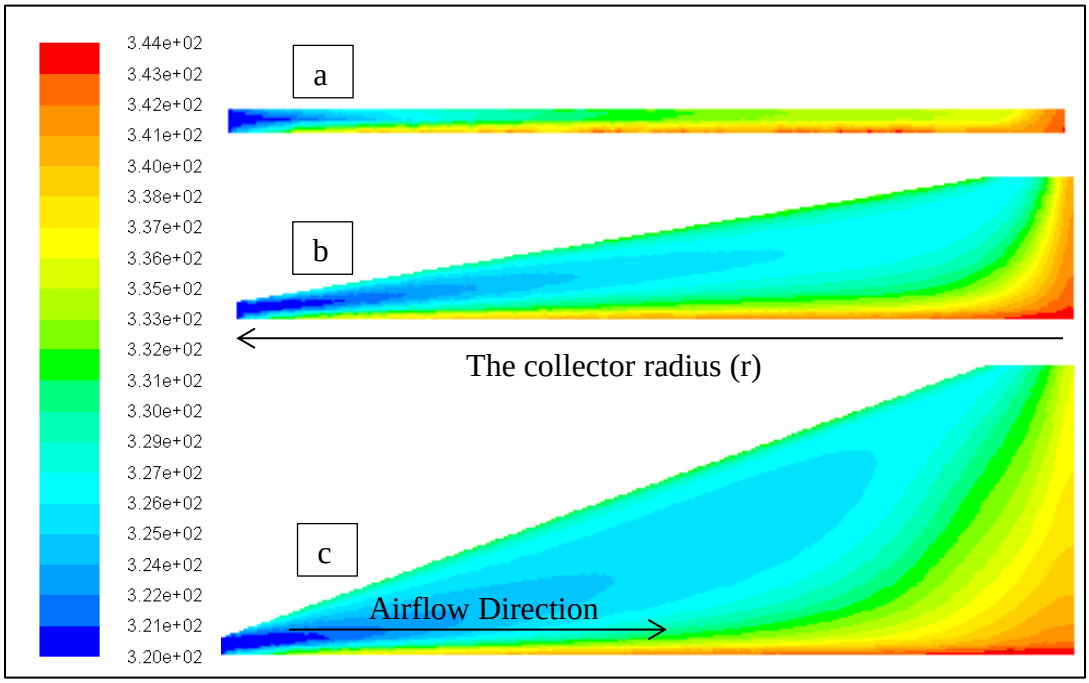

Figure 5. Sectional airflow temperature gradient in the SAC in (K) with inlet height of 0.1 m and inclination angle of (a) 0°, (b) 8.5°, and (c) 20°.

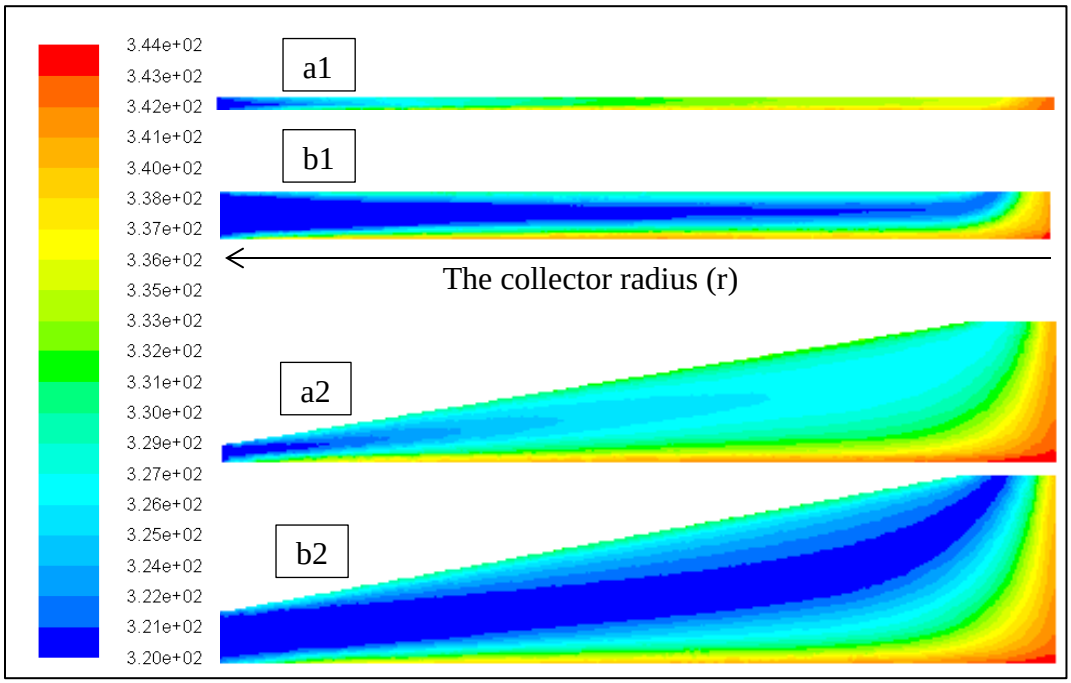

Figure 6. Sectional airflow temperature gradient in the SAC in (K) with inlet height of (a) 0.1 m and (b) 0.25 m, and inclination angle of (1) 0° and (2) 8.5°.

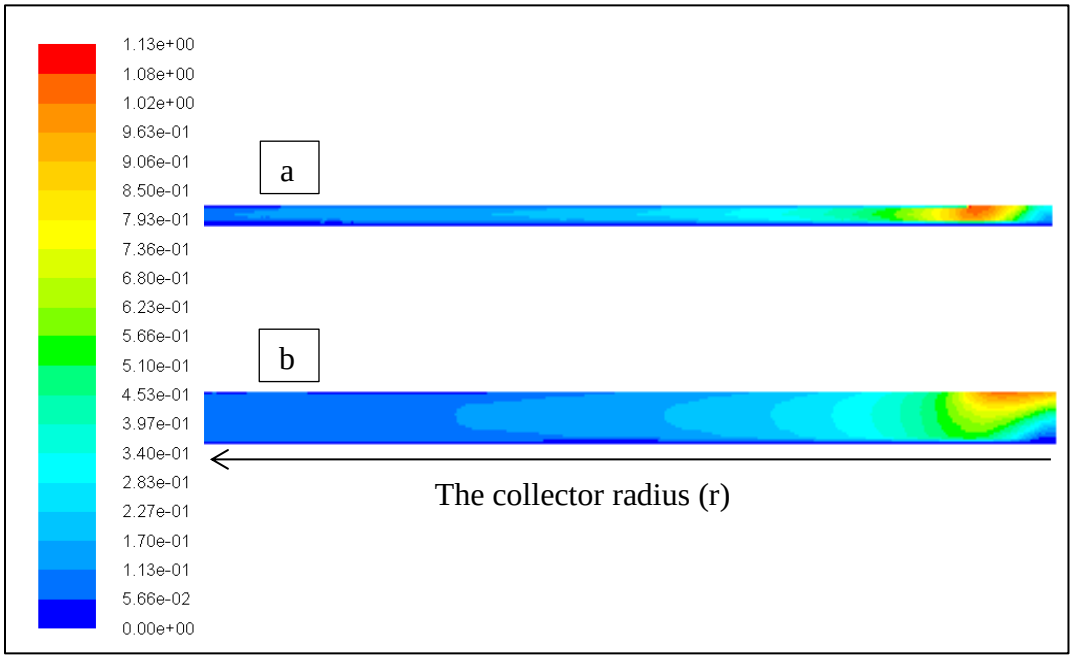

Figure 7. Sectional airflow velocity gradient in the SAC in (m/s) with inclination angle of 0°, and inlet height of (a) 0.1 m and (b) 0.25 m.

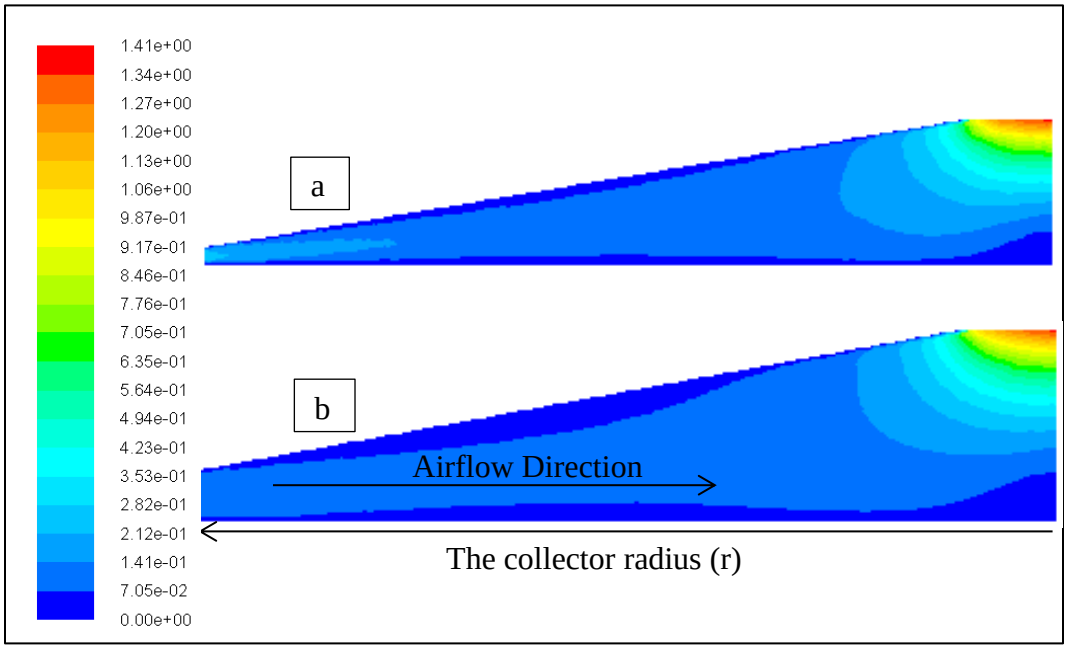

Figure 8. Sectional airflow velocity gradient in the SAC in (m/s) with inclination angle of 8.5°, and inlet height of (a) 0.1 m and (b) 0.25 m.

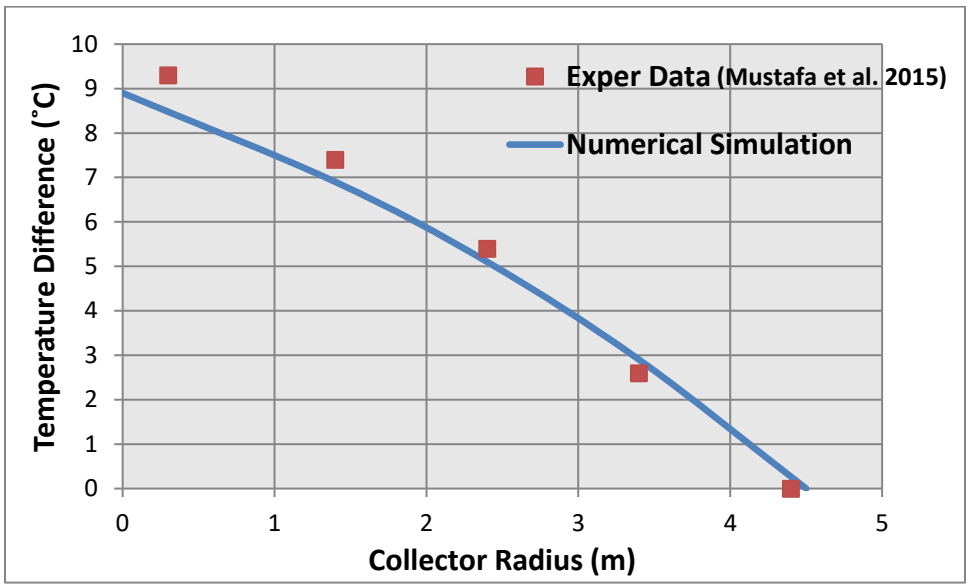

Figure 9. Validation of airflow temperature in the SAC model.